1 **SUPPLEMENTARY MATERIALS**

2

3

4

5 **Photo-induced hydrophilicity at ZnO(11$\overline{2}$0) surface: An evolutionary algorithm**

6 **aided density functional theory study**

7 Shen-Yuan Bao, Dong-Zhi Li and Xue-Qing Gong[*]

8 Key Laboratory for Advanced Materials and Joint International Research Laboratory

9 for Precision Chemistry and Molecular Engineering, Feringa Nobel Prize Scientist

10 Joint Research Center, Centre for Computational Chemistry and Research Institute of

11 Industrial Catalysis, School of Chemistry and Molecular Engineering, East China

12 University of Science and Technology, 130 Meilong Road, Shanghai, 200237, P. R.

13 China.

14 [*]Email: xgong@ecust.edu.cn

15

Session 1. Computational details

Calculation model

The ZnO($11\bar{2}0$) surface was modelled with a 4-layer p(2×2) surface cell. The bottom layer was kept fixed and all the other layers as well as the adsorbates were allowed to relax during the calculations. The vacuum between neighboring slabs was set as 15 Å along the z axis.

DFT calculations

All calculations were performed on the basis of plane-wave Density Functional Theory (DFT) method by using the Vienna ab initio simulation package (VASP) code[1,2]. The functionals used in the calculations were Perdew-Burke-Ernzerhof generalized gradient approximations (GGA-PBE) and strongly constrained and appropriately normed semilocal density functional (meta-GGA SCAN)[3-5]. The core-electron interactions were represented by the project-augmented wave method (PAW[6,7] at a kinetic energy cutoff of 400 eV with Zn (3d, 4s), O (2s, 2p) and H (1s) electrons being treated as valance states. For structure optimization, the ionic positions were allowed to relax until the forces were less than 0.05 eV·Å^{-1}. The Monkhorst-Pack k-point grids were set as $2 \times 2 \times 1$ for all surface cells. The Bader charge and charge difference analyses were used in our work and calculated by SCAN functional.

In this work, the adsorption energy (E_{ads}) was calculated as: $E_{ads} = E_{total} - (E_{opt}^{ZnO} + xE_{opt}^{H_2O})$, where E_{total}, E_{opt}^{ZnO} and $E_{opt}^{H_2O}$ are the total energy of H_2O/ZnO, and the calculated energies of the optimized (non-interacting) ZnO surface and H_2O molecule, respectively, and x is the number of adsorbed H_2O. The average adsorption

energy (E_{ads_adv}) can be obtained as follows: $E_{ads\_adv} = E_{ads}/x$. Therefore, negative

E_{ads} and E_{ads_adv} indicate that the adsorption process is exothermic, and the more

negative, the stronger the adsorption is.

USPEX calculation

The evolutionary algorithm based USPEX (Universal Structure Predictor: Evolutionary Xtallography) package was used in this work[8-10]. The initial population included 10 structures with $64 + 3x$ atoms, where x is the number of adsorbed H_2O. All subsequent generations each consisted of 10 structures produced by heredity (40%), random symmetric generator (20%), permutation (20%) and softmutation (20%). Structure relaxations and total energy calculations were done by the VASP code.

Photo-excited simulation

To simulate the photo-excited states of $ZnO(11\bar{2}0)$ surface and H_2O/ZnO adsorption systems, two methods were adopted in this work by fixing the total spin of the surface system only (Method I) or explicitly specifying the occupations of each spin up and down states (Method II)[11-14]. The calculation details are provided as follows. For Method I, the parameters ISPIN = 2 and NUPDOWN = 2 were used for the system where the difference between the number of spin-up and spin-down electrons was fixed to 2. For Method II, the NBANDS was set as 380, and the electronic occupancies were read from the INCAR file where the parameters FERWE = 289×1.0 91×0.0 and FERDO = 287×1.0 93×0.0.

References

1   [1]   G. Kresse, and J. Hafner, *Phys. Rev. B*, 1993, **47**, 558.

2   [2]   G. Kresse, and J. Hafner, Phys. Rev. B, 1994, **49**, 14251.

3   [3]   J. W. Sun, et al, *Nat. Chem.*, 2016, **8**, 831.

4   [4]   H. W. Peng, Z. H. Yang, J. P. Perdew, and J. W. Sun, *Phys. Rev. X*, 2016, **6**, 041005.

5   [5]   J. W. Sun, A. Ruzsinszky, and J. P. Perdew, *Phys. Rev. Lett.*, 2015, **115**, 036402.

6   [6]   P. E. Blochl, *Phys. Rev. B*, 1994, **50**, 17953.

7   [7]   G. Kresse, and D. Joubert, Phys. Rev. B, 1999, **59**, 1758.

8   [8]   A. O. Lyakhov, A. R. Oganov, H. T. Stokes, and Q. Zhu, *Comput. Phys. Commun.*,

9   2013, **184**, 1172.

10 [9]   A. O. Lyakhov, A. R. Oganov, and M. Valle, *Comput. Phys. Commun.*, 2010, **181**,

11   1623.

12 [10] C. W. Glass, A. R. Oganov, and N. Hansen, *Comput. Phys. Commun.*, 2006, **175**,

13   713.

14 [11] C. Y. Liu, and E. Y. Li, *ACS Appl. Mater. Interfaces*, 2019, **11**, 1638.

15 [12] A. Sajid, J. R. Reimers, and M. J. Ford, *Phys. Rev. B*, 2018, **97**, 064101.

16 [13] C. Y. Liu, and E. Y. Li, *ACS Appl. Energy Mater.*, 2018, **1**, 455.

17 [14] P. Francis, C. Majumder, and S.V. Ghaisas, *Carbon*, 2015, **91**, 358.

18

19

20

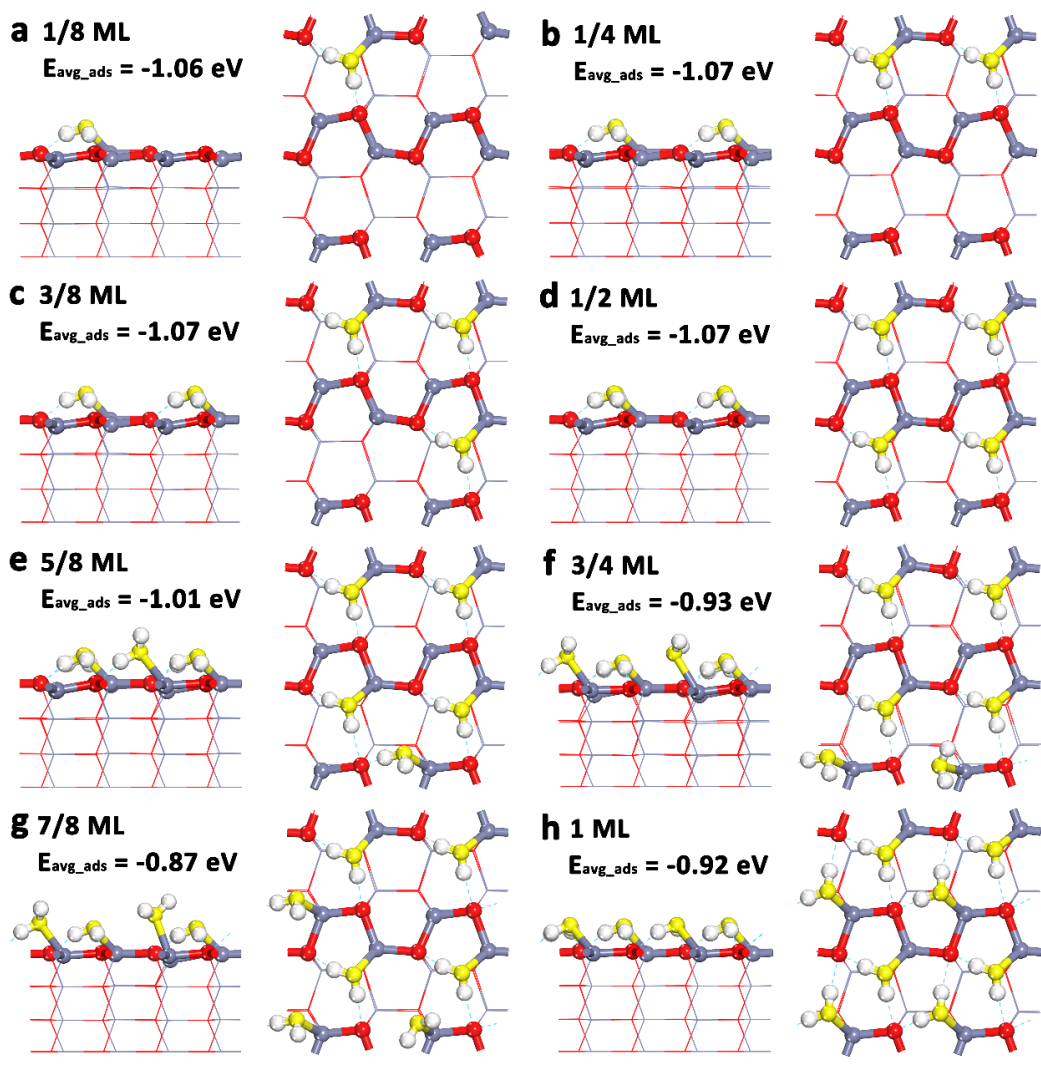**Session 2. Structures of H$_2$O/ZnO with different adsorption configurations and coverages**

In this work, evolutional algorithm aided DFT calculations were adopted to determine the possible structures of H$_2$O/ZnO with different adsorption configurations and under different coverages. Moreover, two electronic exchange-correlation functionals, namely GGA-PBE and meta-GGA SCAN, were applied in the DFT calculations. In Fig. S1-6, we illustrate the relatively most stable structures of H$_2$O/ZnO with molecular, partially and fully dissociative configurations under different coverages obtained through these functionals. By comparing the various calculated structures obtained with different methods (Fig. S1 and S4, Fig. S2 and S5, Fig. S3 and S6), one can see that they are generally quite similar. Nevertheless, since some early studies have suggested that more accurate results about H$_2$O can be obtained by SCAN method, we still used the results from SCAN method for detailed analyses.

The calculated results (see Fig. 1c) suggest that molecular adsorption configurations are more favorable under lower coverages. For better understanding of the reasons, it is necessary to analyze the adsorption and dissociation processes. Taking the structures of 1/8 ML H$_2$O/ZnO as the example (see Fig. S4a and S5a), one can see that for the adsorbed H$_2$O molecule, there exist three O$_{3c}$ (α, β and γ in Fig. S4a) nearby and two of them (α and β) form H-bonds with the H$_2$O. These three O$_{3c}$ may also accommodate the dissociated H after H$_2$O dissociation. However, with the H leaving to site α or β, the dissociated adsorption structures are quite unstable and return to the molecular one. For site γ, although the dissociative H$_2$O adsorption structure with H at

this site can be obtained, the adsorption energy is much worse than that of the molecular

one since the Zn-OH bond is stretched significantly by the H-bonding (see Fig. S5a).

By contrast, when the water coverage rises above 1/2 ML, e.g. 5/8 ML, there would be

no sufficient number of O_{3c} to form H-bonds with every H_2O, as one O_{3c} can only

accommodate one comfortable H-bond. Then, H_2O dissociation may be favored since

it can give rise to surface hydroxyls, the O_{2c} of which can provide more H-bonds for

the co-adsorbed H_2O molecules.

a 1/8 ML
E_{avg_ads} = -1.06 eV

b 1/4 ML
E_{avg_ads} = -1.07 eV

c 3/8 ML
E_{avg_ads} = -1.07 eV

d 1/2 ML
E_{avg_ads} = -1.07 eV

e 5/8 ML
E_{avg_ads} = -1.01 eV

f 3/4 ML
E_{avg_ads} = -0.93 eV

g 7/8 ML
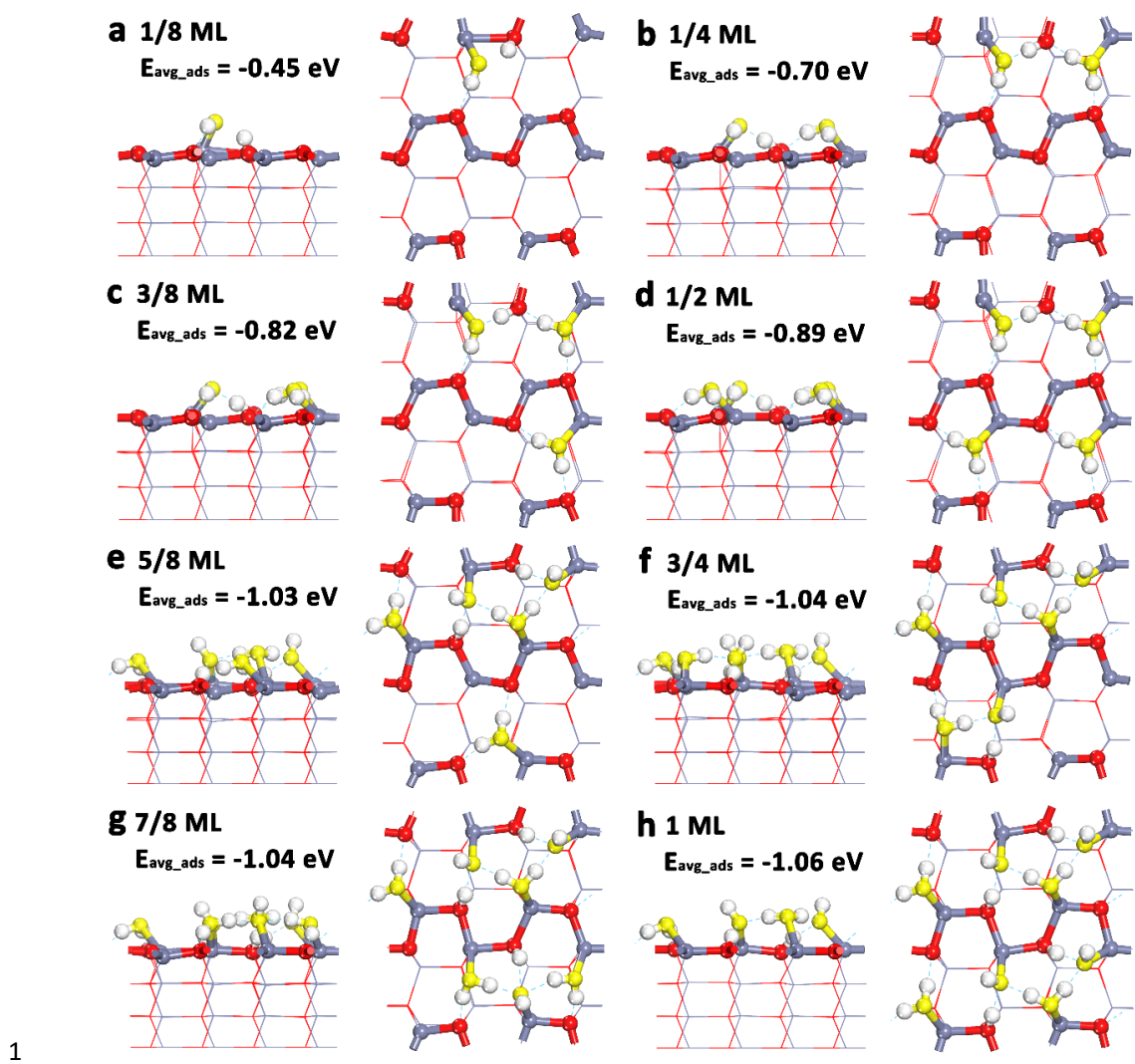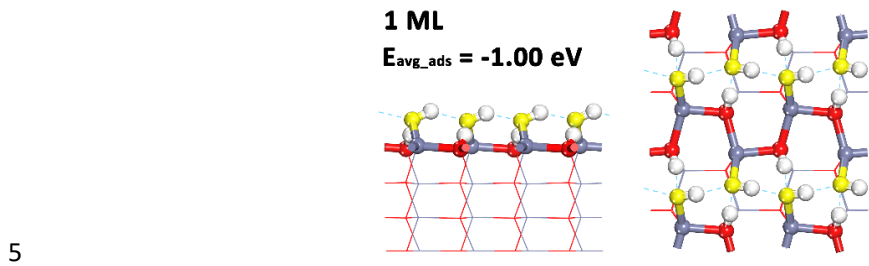E_{avg_ads} = -0.87 eV

h 1 ML
E_{avg_ads} = -0.92 eV

Fig. S1 (a-h) Top (right) and side (left) views of H_2O/ZnO in molecular adsorption configuration under the coverages from 1/8 to 1 ML obtained from PBE calculations.
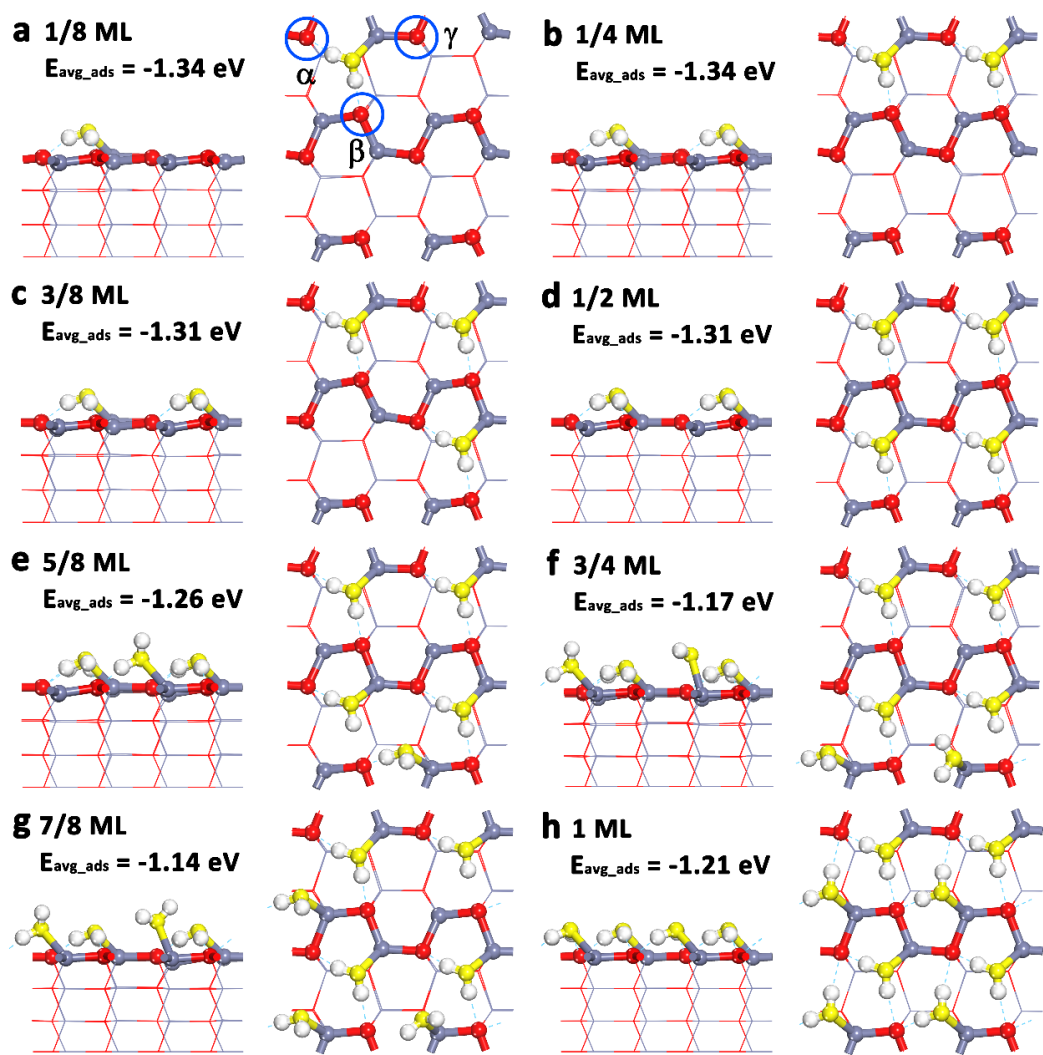
Fig. S2 (a-h) Top (right) and side (left) views of H$_2$O/ZnO in partially dissociative adsorption configurations under the coverages from 1/8 to 1 ML obtained from PBE calculations.

Fig. S3 Top (right) and side (left) views of 1 ML H$_2$O/ZnO in fully dissociative adsorption configuration obtained from PBE calculations.

a 1/8 ML
E_{avg_ads} = -1.34 eV

b 1/4 ML
E_{avg_ads} = -1.34 eV

c 3/8 ML
E_{avg_ads} = -1.31 eV

d 1/2 ML
E_{avg_ads} = -1.31 eV

e 5/8 ML
E_{avg_ads} = -1.26 eV

f 3/4 ML
E_{avg_ads} = -1.17 eV

g 7/8 ML
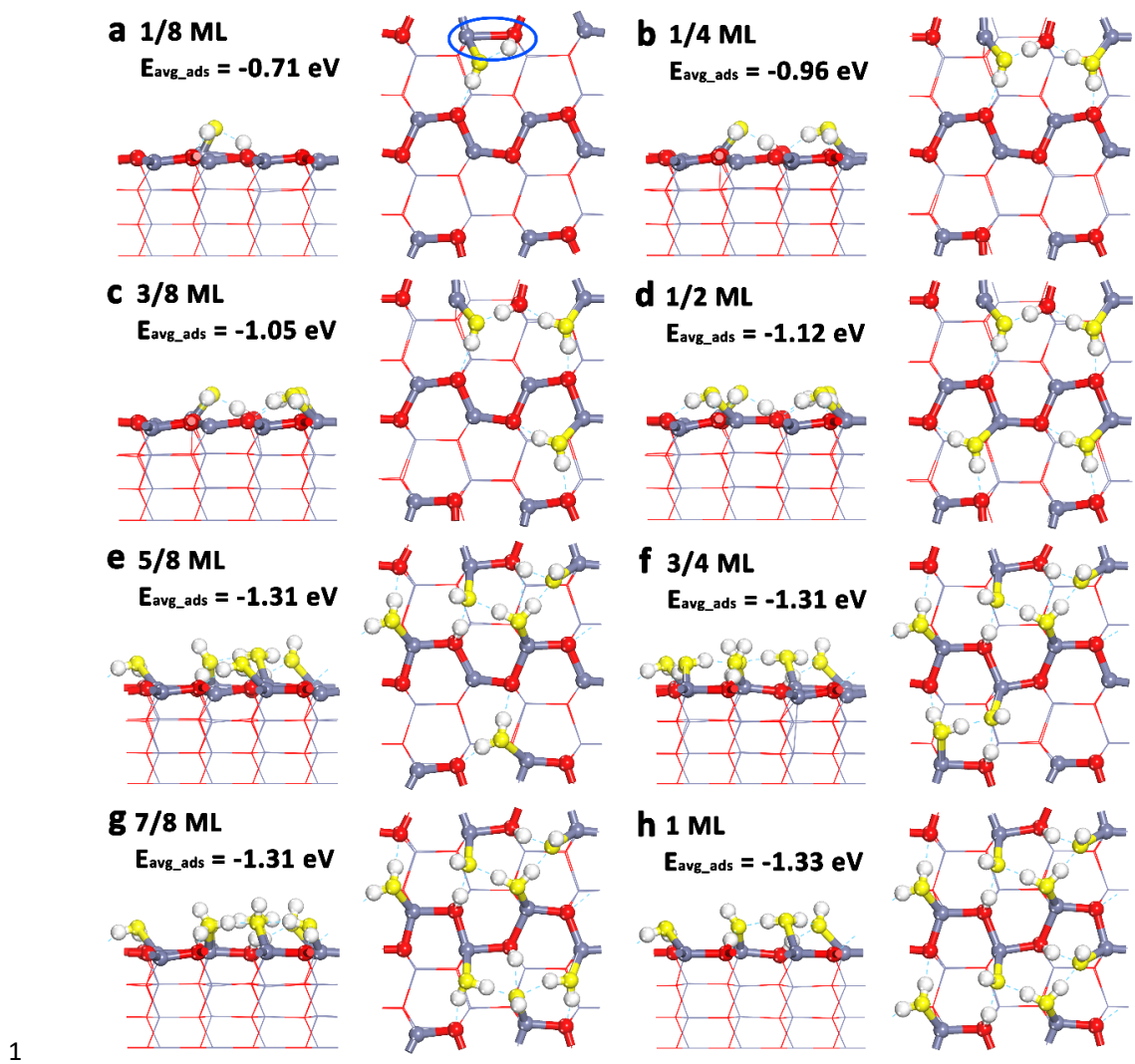E_{avg_ads} = -1.14 eV

h 1 ML
E_{avg_ads} = -1.21 eV

Fig. S4 (a-h) Top (right) and side (left) views of H_2O/ZnO in molecular adsorption configurations under the coverages from 1/8 to 1 ML obtained from SCAN calculations.

a 1/8 ML
E_{avg_ads} = -0.71 eV

b 1/4 ML
E_{avg_ads} = -0.96 eV

c 3/8 ML
E_{avg_ads} = -1.05 eV

d 1/2 ML
E_{avg_ads} = -1.12 eV

e 5/8 ML
E_{avg_ads} = -1.31 eV

f 3/4 ML
E_{avg_ads} = -1.31 eV

g 7/8 ML
E_{avg_ads} = -1.31 eV

h 1 ML
E_{avg_ads} = -1.33 eV

Fig. S5 (a-h) Top (right) and side (left) views of H_2O/ZnO in partially dissociative adsorption configurations under the coverages from 1/8 to 1 ML obtained from SCAN calculations.

1 ML
E_{avg_ads} = -1.33 eV
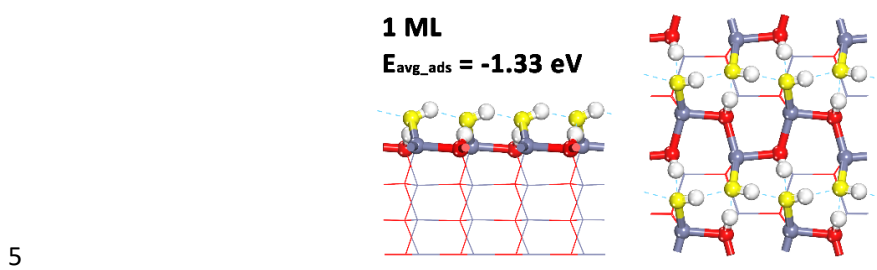
Fig. S6 Top (right) and side (left) views of 1 ML H_2O/ZnO in fully dissociative adsorption configuration obtained from SCAN calculations.

Session 3. Energetic and electronic analyses

In Fig. S7-16, we illustrate the calculated structures and energy decomposition results of H_2O/ZnO under different water coverages. Fig. S17 shows the calculated average distortion energies of H_2O in molecular and dissociative adsorption configurations under different coverages. In Fig. S18-20, we also calculated the electronic charge redistributions between the various H_2O and the surface, between the various H_2O and the rest adsorbed H_2O, among the various H_2O, the rest adsorbed H_2O and the ZnO surface of *1-pd* H_2O/ZnO. The calculation processes and results of each component are discussed as following.

We tentatively suggest that the total energy (E_{total}) of the interacting H_2O/ZnO system can be decomposed into altogether seven components according to the different natures of the interactions,

$$E_{total} = E_{opt}^{ZnO} + x E_{opt}^{H_2O} + E_{distort}^{ZnO}$$

$$+ \sum_{i=1}^{x} (E_{distort}^{H_2O(i)} + E_{int}^{H_2O(i)/ZnO} + \frac{1}{2} E_{int}^{H_2O(i)/H_2O(x-i)} + \frac{1}{2} E_{int-indirect}^{H_2O(i)})$$

where x is the number of adsorbed H_2O; i represents the interested H_2O ($H_2O(i)$); E_{opt}^{ZnO} and $E_{opt}^{H_2O}$ are the calculated energies of the optimized (non-interacting) ZnO surface and H_2O molecule, respectively; $E_{distort}^{ZnO}$ and $E_{distort}^{H_2O(i)}$ represent the distortion energies of the ZnO surface and adsorbed $H_2O(i)$ upon adsorption; $E_{int}^{H_2O(i)/ZnO}$ and $E_{int}^{H_2O(i)/H_2O(x-i)}$ represent the direct interaction energies between $H_2O(i)$ and ZnO surface and the rest adsorbed H_2O molecules, respectively; and $E_{int-indirect}^{H_2O(i)}$ is defined as the indirect interaction energy among $H_2O(i)$, the rest H_2O molecules and ZnO surface.

Distortion energies of the ZnO(11$\bar{2}$0) surfaces

The distortion energies of the ZnO(11$\bar{2}$0) surface were obtained by

$$E_{distort}^{ZnO} = E_{sp}^{ZnO} - E_{opt}^{ZnO}$$

where E_{sp}^{ZnO} is the calculated single point energy of the ZnO surface in H_2O/ZnO; E_{opt}^{ZnO}

is the calculated energy of the optimized (non-interacting) ZnO surface.

Distortion energies of H$_2$O

Similar to $E_{distort}^{ZnO}$, the distortion energies of H_2O molecules can be calculated as,

$$E_{distort}^{H_2O(i)} = E_{sp}^{H_2O(i)} - E_{opt}^{H_2O}$$

where $E_{sp}^{H_2O(i)}$ is the calculated single point energy of the interested H_2O in the

adsorption state; $E_{opt}^{H_2O}$ is the calculated energy of the optimized (non-interacting) H_2O.

As shown in Fig. S17, $E_{distort}^{H_2O(i)}$ is only relied on the adsorption configuration. For the

adsorbed molecular H_2O, $E_{distort}^{H_2O(i)}$ were calculated to be ~0.08 eV, and much larger

energies (above 3.00 eV) were obtained for the dissociated ones.

Interaction energies between H$_2$O*(i)* and ZnO surface

The interaction energies between H_2O*(i)* and ZnO surface $(E_{int}^{H_2O(i)/ZnO})$ largely

depend on the chemical bonds and H-bonds, and can be calculated as,

$$E_{int}^{H_2O(i)/ZnO} = E_{sp}^{H_2O(i)/ZnO} - E_{sp}^{H_2O(i)} - E_{sp}^{ZnO}$$

where $E_{sp}^{H_2O(i)/ZnO}$, $E_{sp}^{H_2O(i)}$ and E_{sp}^{ZnO} are the calculated single point energies of the

ZnO surface containing H_2O*(i)*, interested H_2O and ZnO surface in H_2O/ZnO.

Similarly, the electron redistribution (Fig. S18) between H_2O*(i)* and ZnO surface

$(D_{int}^{H_2O(i)/ZnO})$ in *1-pd* H_2O/ZnO can be calculated as,

$$D_{int}^{H_2O(i)/ZnO} = D^{H_2O(i)/ZnO} - D^{H_2O(i)} - D^{ZnO}$$

where $D^{H_2O(i)/ZnO}$, $D^{H_2O(i)}$ and D^{ZnO} are the electron distribution of the ZnO surface

containing $H_2O(i)$, interested H_2O and ZnO surface in *1-pd* H_2O/ZnO.

For most H_2O in molecular adsorption configuration, one O_{H_2O}-Zn_{3c} bond and

two H-bonds are formed between these H_2O molecules and the ZnO surface, and

$E_{int}^{H_2O(i)/ZnO}$ were calculated to be ~-1.55 eV. While the $E_{int}^{H_2O(i)/ZnO}$ of H_2O in

dissociative adsorption configuration are much larger (~5.00 eV), due to the stronger

interaction between H_2O and ZnO through O_{H_2O}-Zn_{3c} and H_{H_2O}-O_{3c} bonds. The same

trend can be also found in the electron redistribution between $H_2O(i)$ and ZnO surface

in *1-pd* H_2O/ZnO (see in Fig. S18).

Interaction energies between $H_2O(i)$ and the rest adsorbed H_2O

The interaction energies between $H_2O(i)$ and the rest adsorbed H_2O

($E_{int}^{H_2O(i)/H_2O(x-i)}$) are mainly determined by the H-bonding and electrostatic

interactions in between, and can be calculated as,

$$E_{int}^{H_2O(i)/H_2O(x-i)} = E_{sp}^{H_2O(i)/H_2O(x-i)} - E_{sp}^{H_2O(i)} - E_{sp}^{H_2O(x-i)}$$

where $E_{sp}^{H_2O(i)/H_2O(x-i)}$, $E_{sp}^{H_2O(i)}$ and $E_{sp}^{H_2O(x-i)}$ are the calculated single point energies

of the adsorbed H_2O layer, the interested H_2O and the rest adsorbed H_2O, respectively.

The electron redistribution (Fig. S19) between $H_2O(i)$ and the rest adsorbed H_2O

$(D_{int}^{H_2O(i)/H_2O(x-i)})$ in *1-pd* H_2O/ZnO can be calculated as,

$$D_{int}^{H_2O(i)/H_2O(x-i)} = D^{H_2O(i)/H_2O(x-i)} - D^{H_2O(i)} - D^{H_2O(x-i)}$$

where $D^{H_2O(i)/H_2O(x-i)}$, $D^{H_2O(i)}$ and $D^{H_2O(x-i)}$ are the electron distribution of the adsorbed H_2O layer, the interested H_2O and the rest adsorbed H_2O.

According to the calculated results, under low coverages, the distances between each H_2O are too large (> 5 Å) and the corresponding $E_{int}^{H_2O(i)/H_2O(x-i)}$ can be neglected. For the separate H_2O in the 1×3 configuration of the partially dissociative adsorption structure under 1 ML, it has no H-bond with other H_2O, but there still exist weak interactions ($E_{int}^{H_2O(i)/H_2O(x-i)}$ = -0.23 eV) which can attributed to the electrostatic interaction (see Fig. S19a and b). For the H_2O molecule within the cluster of such 1×3 configuration, it connects with the rest dissociated H_2O by H-bonds ($E_{int}^{H_2O(i)/H_2O(x-i)}$ = -0.35 eV), and significant electron redistributions can be also recognized (see Fig. S19c-h).

Indirect interaction energies among H_2O*(i)*, the rest adsorbed H_2O molecules and ZnO surface

Indirect interaction energy among H_2O*(i)*, the rest adsorbed H_2O molecules and ZnO surface ($E_{int-indirect}^{H_2O(i)}$) can be generally ascribed to electron redistribution caused by the adsorptions. It can be calculated as,

$$E_{int-indirect}^{H_2O(i)} = E_{total} - E_{sp}^{ZnO} - E_{sp}^{H_2O(i)} - E_{sp}^{H_2O(x-i)} - E_{int}^{H_2O(i)/H_2O(x-i)}$$
$$- E_{int}^{H_2O(i)/ZnO} - E_{int}^{H_2O(x-i)/ZnO}$$

where E_{total} is the calculated total energy of the adsorption system; E_{sp}^{ZnO}, $E_{sp}^{H_2O(i)}$ and $E_{sp}^{H_2O(x-i)}$ are the calculated single point energies of ZnO surface, the interested H_2O and the rest adsorbed H_2O in the adsorption state; $E_{int}^{H_2O(i)/H_2O(x-i)}$, $E_{int}^{H_2O(i)/ZnO}$ and

1     $E_{int}^{H_2O(x-i)/ZnO}$ are the interaction energies between the interested H_2O and the rest

2   adsorbed H_2O, between the interested H_2O and ZnO surface and between the rest

3   adsorbed H_2O molecules and ZnO surface, respectively.

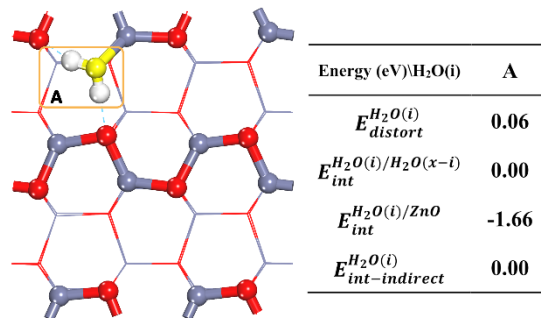4   The electron redistribution (Fig. S20) among $H_2O(i)$, the rest adsorbed H_2O

5   molecules and ZnO surface ($D_{int-indirect}^{H_2O(i)}$) in *1-pd* H_2O/ZnO can be calculated as,

6     $$D_{int-indirect}^{H_2O(i)} = D_{total} - D^{ZnO} - D^{H_2O(i)} - D^{H_2O(x-i)} - D_{int}^{H_2O(i)/H_2O(x-i)}$$

7     $$- D_{int}^{H_2O(i)/ZnO} - D_{int}^{H_2O(x-i)/ZnO}$$

8   where D_{total} is the electron distribution of *1-pd* H_2O/ZnO; D^{ZnO}, $D^{H_2O(i)}$ and

9     $D^{H_2O(x-i)}$ are the electron distribution of ZnO surface, the interested H_2O and the rest

10   adsorbed H_2O in the adsorption state; $D_{int}^{H_2O(i)/H_2O(x-i)}$, $D_{int}^{H_2O(i)/ZnO}$ and $D_{int}^{H_2O(x-i)/ZnO}$

11   are the electron redistribution between the interested H_2O and the rest adsorbed H_2O,

12   between the interested H_2O and ZnO surface and between the rest adsorbed H_2O

13   molecules and ZnO surface in *1-pd* H_2O/ZnO.

14   As shown in Fig. S20a and b, rather small electronic charge redistributions of the

15   separate H_2O in the 1×3 configuration was detected. However, for the H_2O molecules

16   in the cluster, their electronic charge redistributions are much larger (see Fig. S20c-h),

17   suggesting the higher $E_{int-indirect}^{H_2O(i)}$ (see in Fig. S15).

18

Energy (eV)\\$H_2O(i)$	A
$E_{distort}^{H_2O(i)}$	0.06
$E_{int}^{H_2O(i)/H_2O(x-i)}$	0.00
$E_{int}^{H_2O(i)/ZnO}$	-1.66
$E_{int-indirect}^{H_2O(i)}$	0.00

19

1　Fig. S7 Calculated structure and energy decomposition results of *1/8-m* H_2O/ZnO.

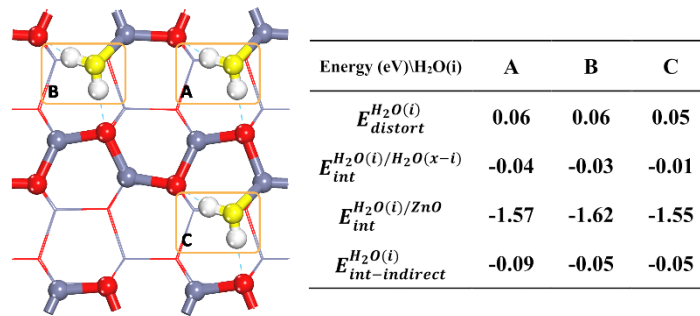| Energy (eV)\ $H_2O(i)$	A	B
$E_{distort}^{H_2O(i)}$	0.07	0.07
$E_{int}^{H_2O(i)/H_2O(x-i)}$	-0.03	-0.03
$E_{int}^{H_2O(i)/ZnO}$	-1.64	-1.63
$E_{int-indirect}^{H_2O(i)}$	-0.05	-0.05
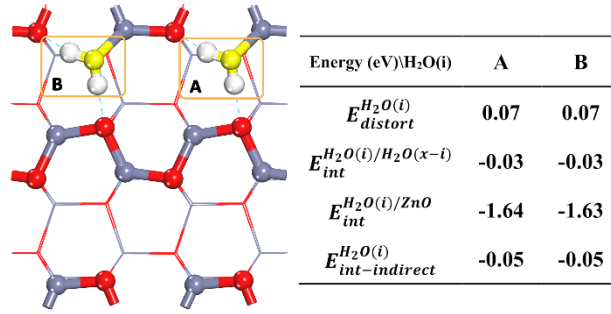
2

3　Fig. S8 Calculated structure and energy decomposition results of *1/4-m* H_2O/ZnO.

Energy (eV)\ $H_2O(i)$	A	B	C
$E_{distort}^{H_2O(i)}$	0.06	0.06	0.05
$E_{int}^{H_2O(i)/H_2O(x-i)}$	-0.04	-0.03	-0.01
$E_{int}^{H_2O(i)/ZnO}$	-1.57	-1.62	-1.55
$E_{int-indirect}^{H_2O(i)}$	-0.09	-0.05	-0.05

4

5　Fig. S9 Calculated structure and energy decomposition results of *3/8-m* H_2O/ZnO.

Energy (eV)\ $H_2O(i)$	A	B	C	D
$E_{distort}^{H_2O(i)}$	0.06	0.06	0.05	0.05
$E_{int}^{H_2O(i)/H_2O(x-i)}$	-0.04	-0.04	-0.04	-0.04
$E_{int}^{H_2O(i)/ZnO}$	-1.56	-1.56	-1.56	-1.55
$E_{int-indirect}^{H_2O(i)}$	-0.09	-0.09	-0.08	-0.08
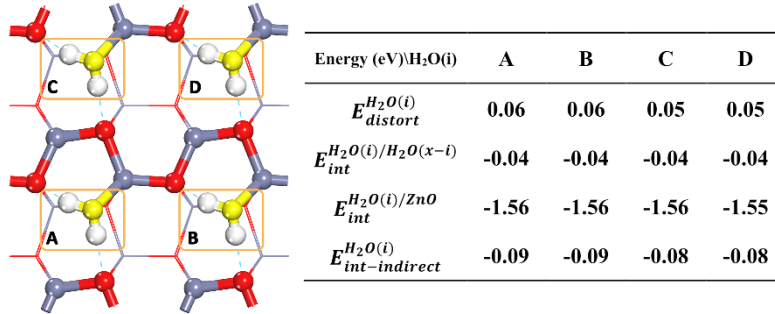
6

7　Fig. S10 Calculated structure and energy decomposition results of *1/2-m* H_2O/ZnO.

Energy (eV)\ $H_2O(i)$	A	B	C	D	E
$E_{distort}^{H_2O(i)}$	0.07	3.21	0.06	3.71	0.11
$E_{int}^{H_2O(i)/H_2O(x-i)}$	-0.07	-0.41	-0.23	-0.39	-0.52
$E_{int}^{H_2O(i)/ZnO}$	-1.57	-4.77	-1.47	-5.04	-1.02
$E_{int-indirect}^{H_2O(i)}$	-0.06	-0.65	-0.23	-0.78	-0.71
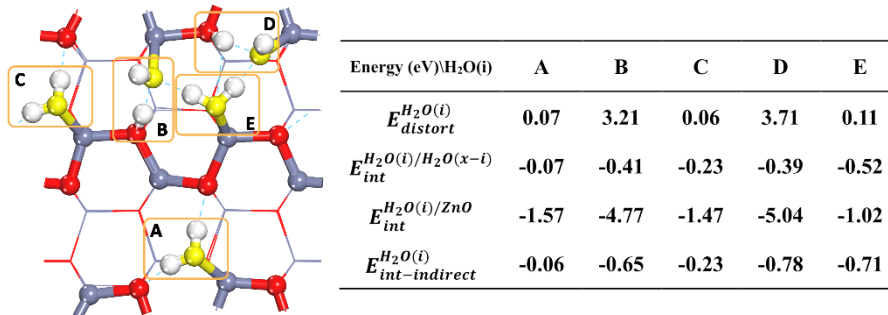
8

9　Fig. S11 Calculated structure and energy decomposition results of *5/8-pd* H_2O/ZnO.
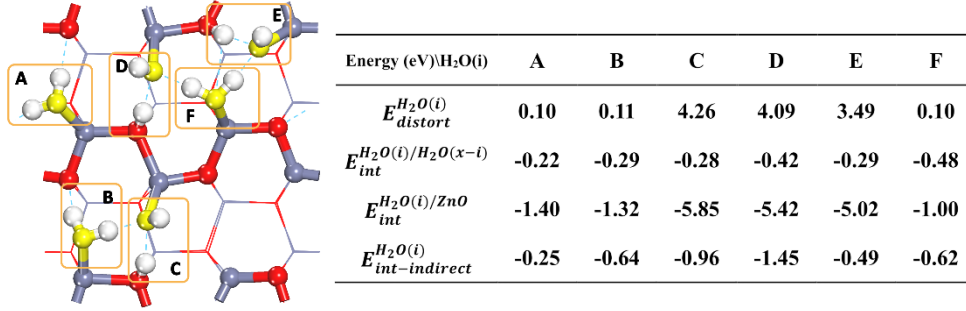
Energy (eV)\\$H_2O(i)$	A	B	C	D	E	F
$E_{distort}^{H_2O(i)}$	0.10	0.11	4.26	4.09	3.49	0.10
$E_{int}^{H_2O(i)/H_2O(x-i)}$	-0.22	-0.29	-0.28	-0.42	-0.29	-0.48
$E_{int}^{H_2O(i)/ZnO}$	-1.40	-1.32	-5.85	-5.42	-5.02	-1.00
$E_{int-indirect}^{H_2O(i)}$	-0.25	-0.64	-0.96	-1.45	-0.49	-0.62

Fig. S12 Calculated structure and energy decomposition results of 3/4-pd H_2O/ZnO.

Energy (eV)\\$H_2O(i)$	A	B	C	D	E	F	G
$E_{distort}^{H_2O(i)}$	0.10	0.12	0.06	3.90	3.92	5.05	0.12
$E_{int}^{H_2O(i)/H_2O(x-i)}$	-0.19	-0.32	-0.22	-0.14	-0.57	-0.57	-0.62
$E_{int}^{H_2O(i)/ZnO}$	-1.38	-1.23	-1.44	-5.23	-5.34	-6.28	-0.89
$E_{int-indirect}^{H_2O(i)}$	-0.30	-0.72	-0.21	-1.05	-0.95	-1.34	-0.82
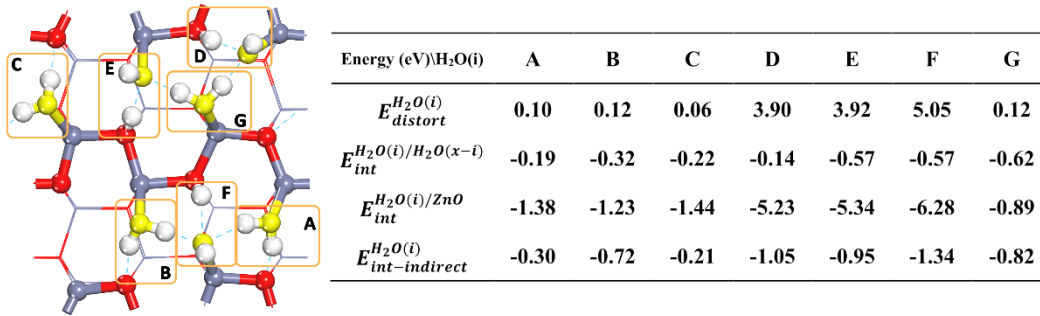
Fig. S13 Calculated structure and energy decomposition results of 7/8-pd H_2O/ZnO.

Energy (eV)\\$H_2O(i)$	A	B	C	D	E	F	G	H
$E_{distort}^{H_2O(i)}$	0.09	0.07	0.08	0.08	0.08	0.07	0.08	0.09
$E_{int}^{H_2O(i)/H_2O(x-i)}$	-0.03	-0.03	-0.03	-0.04	-0.03	-0.01	-0.02	-0.05
$E_{int}^{H_2O(i)/ZnO}$	-1.45	-1.41	-1.42	-1.41	-1.42	-1.45	-1.45	-1.43
$E_{int-indirect}^{H_2O(i)}$	-0.05	-0.03	-0.05	-0.04	-0.04	-0.05	-0.04	-0.04
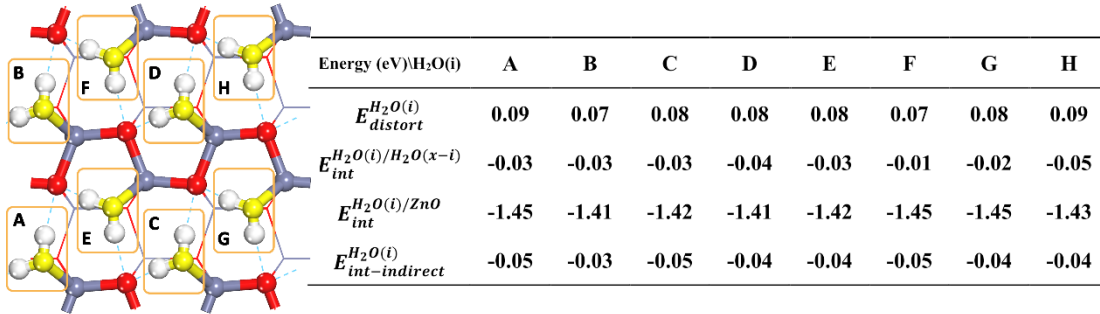
Fig. S14 Calculated structure and energy decomposition results of 1-m H_2O/ZnO.

Energy (eV)\\$H_2O(i)$	A	B	C	D	E	F	G	H
$E_{distort}^{H_2O(i)}$	0.08	0.09	4.17	4.17	3.58	3.55	0.12	0.12
$E_{int}^{H_2O(i)/H_2O(x-i)}$	-0.24	-0.24	-0.36	-0.36	-0.54	-0.46	-0.61	-0.61
$E_{int}^{H_2O(i)/ZnO}$	-1.44	-1.44	-5.60	-5.60	-5.04	-5.00	-0.92	-0.91
$E_{int-indirect}^{H_2O(i)}$	-0.28	-0.29	-1.37	-1.36	-0.51	-0.60	-0.79	-0.79
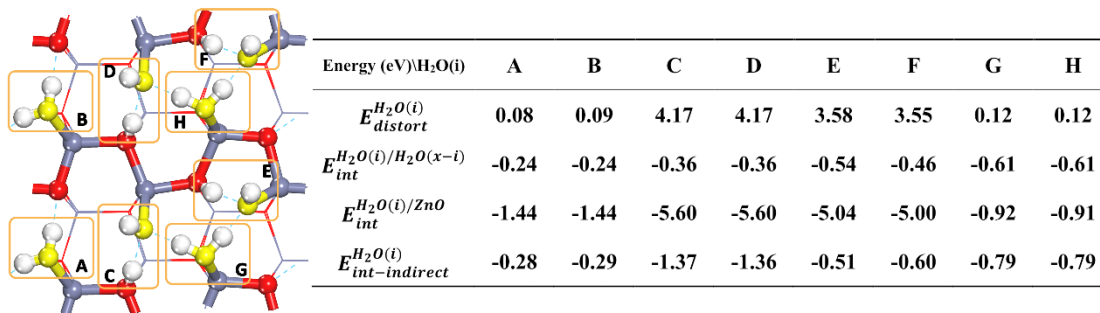
Fig. S15 Calculated structure and energy decomposition results of 1-pd H_2O/ZnO.

Energy (eV)\\$H_2O(i)$	A	B	C	D	E	F	G	H
$E_{distort}^{H_2O(i)}$	3.22	3.22	3.31	3.31	3.32	3.32	3.28	3.28
$E_{int}^{H_2O(i)/H_2O(x-i)}$	-0.65	-0.65	-0.64	-0.64	-0.64	-0.64	-0.65	-0.65
$E_{int}^{H_2O(i)/ZnO}$	-4.57	-4.57	-4.73	-4.73	-4.70	-4.70	-4.67	-4.67
$E_{int-indirect}^{H_2O(i)}$	-0.82	-0.82	-0.80	-0.80	-0.81	-0.81	-0.81	-0.81
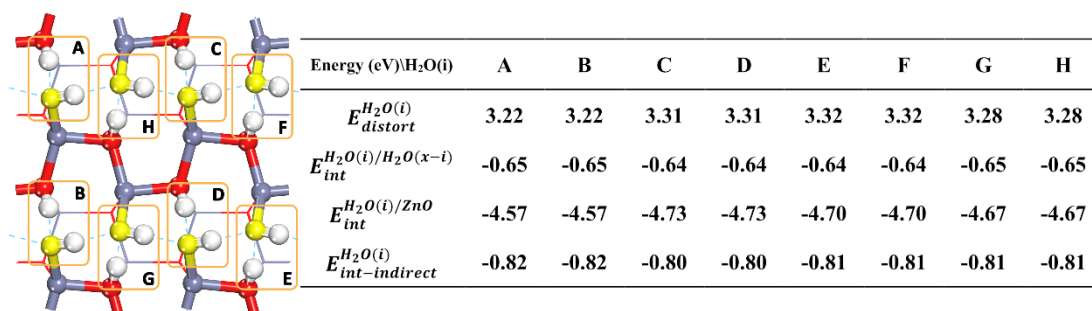
1

2   Fig. S16 Calculated structure and energy decomposition results of *1-fd* H_2O/ZnO.
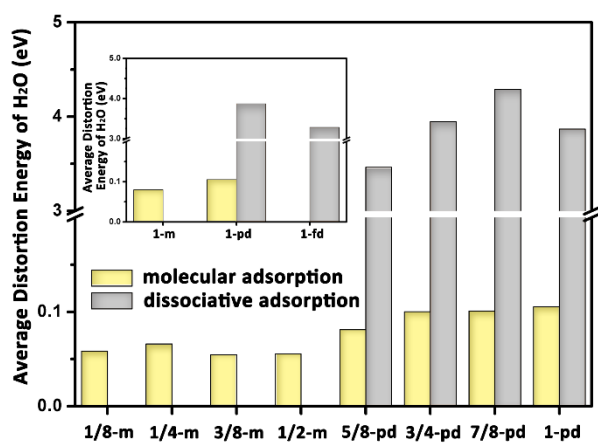
3

4   Fig. S17 Calculated average distortion energies of H_2O in molecular and dissociative

5   adsorption configurations under different coverages.
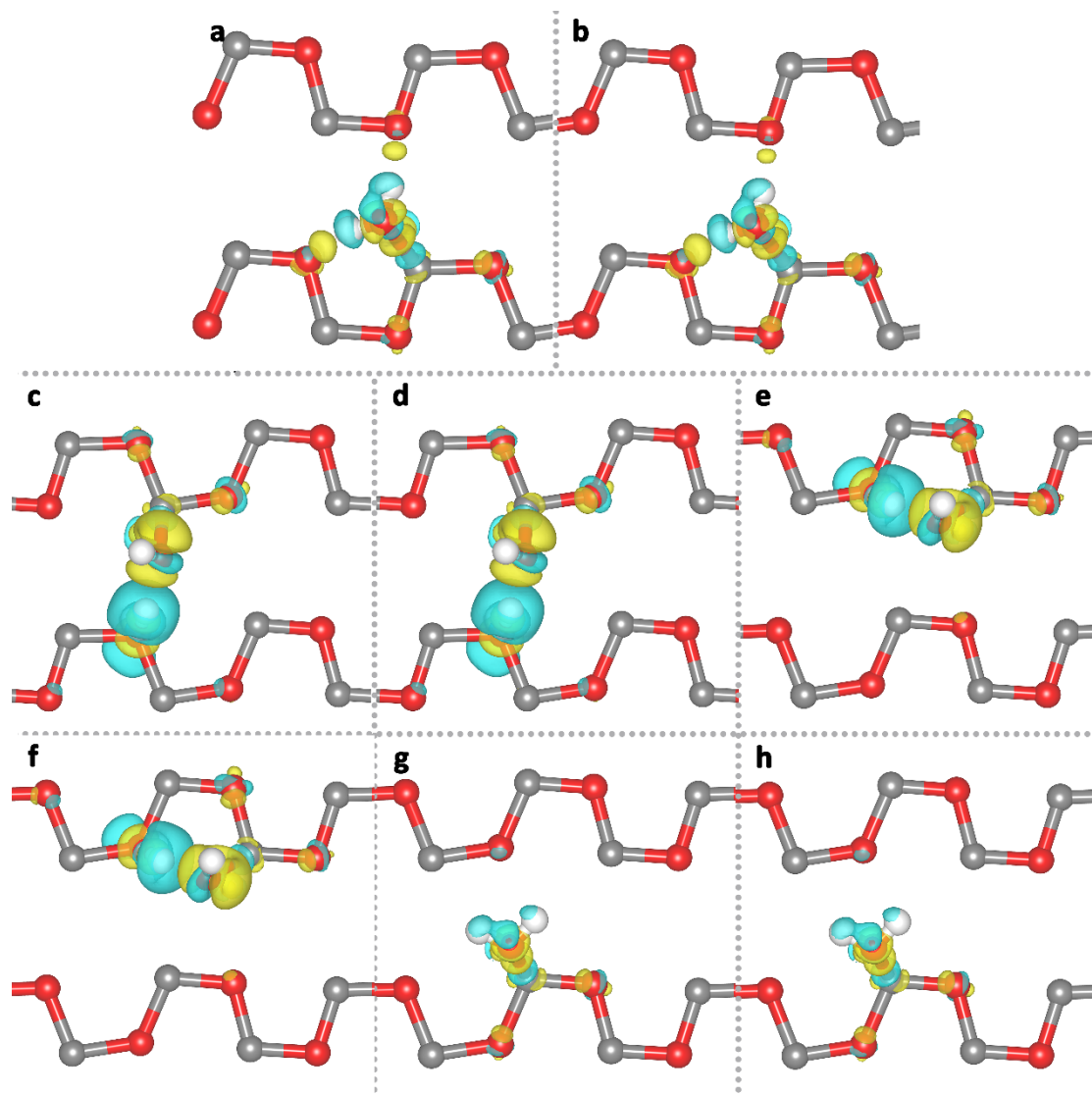
Fig. S18 Calculated electronic charge redistributions between the various H_2O and the surface in *1-pd* H_2O/ZnO. (a-h) The adsorbed H_2O A-H (see Fig. S15).
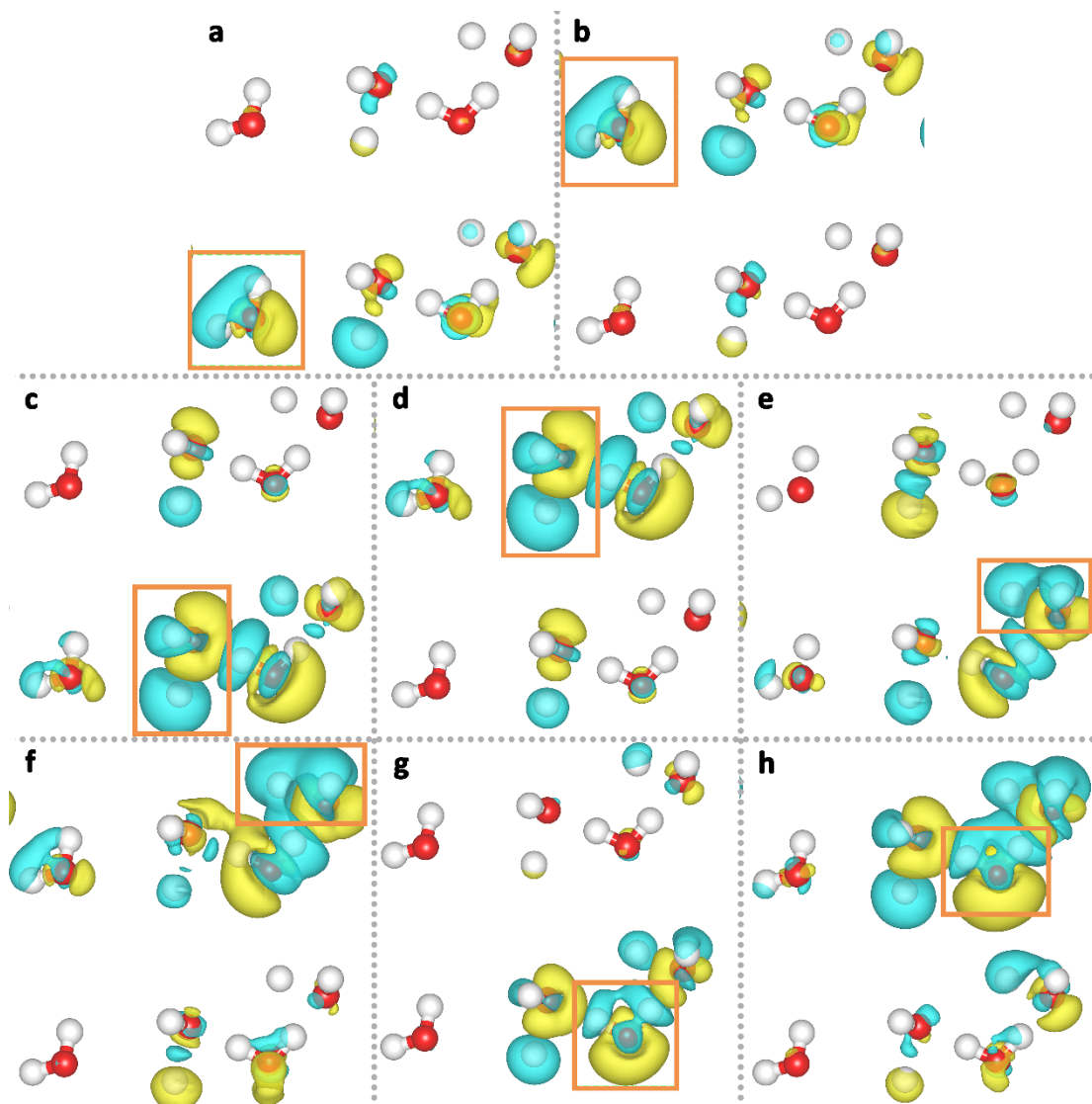
Fig. S19 Calculated electronic charge redistributions between the various H_2O and the rest adsorbed H_2O of *1-pd* H_2O/ZnO. (a-h) The solid rectangle in orange represents the interested H_2O A-H (see Fig. S15).
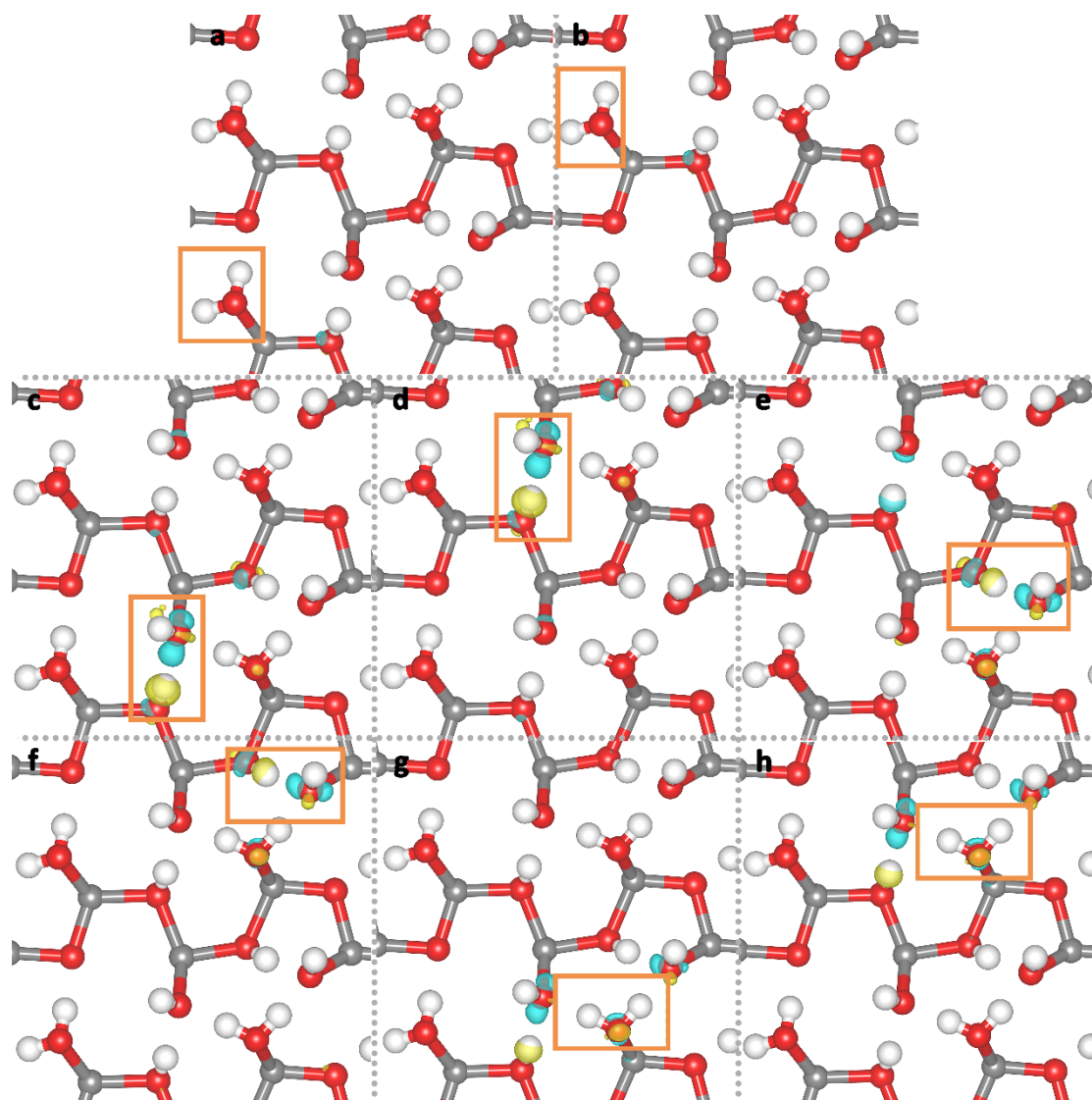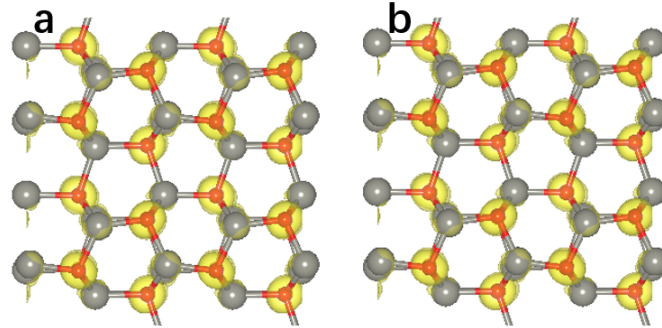
Fig. S20 Calculated electronic charge redistributions among the various H_2O, the rest

adsorbed H_2O and the ZnO surface of *1-pd* H_2O/ZnO. (a-h) The solid rectangle in
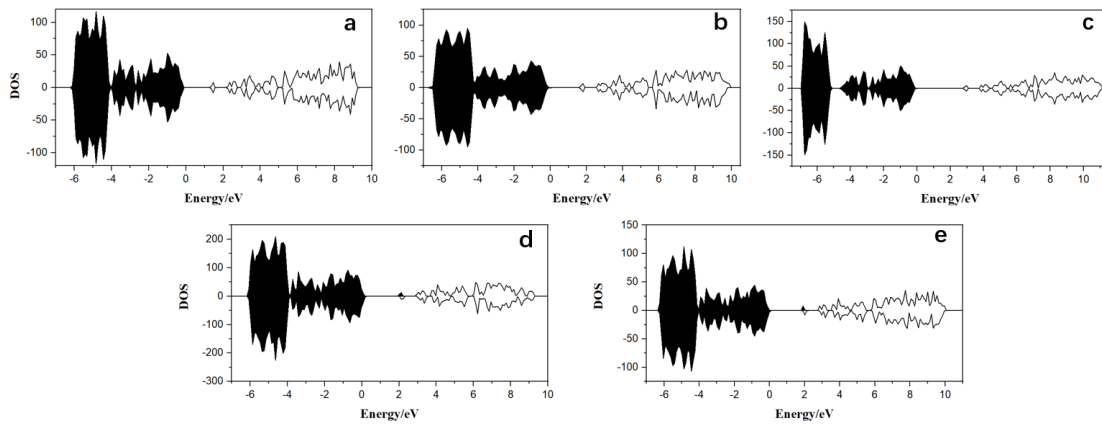
orange represents the interested H_2O A-H (see Fig. S15).

Session 4. Calculated spin charge density and DOS after re-adjusting the location of one electron at the Fermi level

Fig. S21 Calculated spin charge density (in yellow) of the ZnO(11$\bar{2}$0) at excited state by method I (a) and method II (b).

Fig. S22 Calculated DOS of the ZnO(11$\bar{2}$0) surface slab at ground state by (a) PBE, (b) SCAN and (c) HSE06, and excited state simulated with (d) method I and (e) method II by SCAN. The occupied and empty states are filled in black and empty, respectively.

Session 5. Calculated electronic charge redistributions after re-adjusting the location of one electron at the Fermi level

Table SI Electronic charge redistributions within $ZnO(11\bar{2}0)$ of *1-m*, *1-pd* and *1-fd* H_2O/ZnO after re-adjusting the location of one electron at the Fermi level by Method I and Method II. $\Delta_{electron}$ represents the difference between electronic charges of O and Zn before and after the re-adjusting. In this table, all data were calculated by Bader charges.

	electron amount in O (e)	electron amount in Zn (e)	$\Delta_{electron}$
optimized ZnO (original state)	231.26	344.74	/
optimized ZnO (Method I)	231.18	344.82	0.08
optimized ZnO (Method II)	231.15	344.85	0.11
1-m H_2O/ZnO (original state)	230.82	345.18	/
1-m H_2O/ZnO (Method I)	230.46	345.54	0.36
1-m H_2O/ZnO (Method II)	230.47	345.53	0.35
1-pd H_2O/ZnO (original state)	231.00	345.00	/
1-pd H_2O/ZnO (Method I)	230.71	345.29	0.29
1-pd H_2O/ZnO (Method II)	230.72	345.28	0.28
1-fd H_2O/ZnO (original state)	231.00	345.00	/
1-fd H_2O/ZnO (Method I)	230.72	345.28	0.28
1-fd H_2O/ZnO (Method II)	230.73	345.27	0.27